AIP | Journal of Applied Physics

Controlling the Goos-Hänchen shift with external electric and magnetic fields in an electro-optic/magneto-electric heterostructure

Yu. S. Dadoenkova, F. F. L. Bentivegna, N. N. Dadoenkova, R. V. Petrov, I. L. Lyubchanskii, and M. I. Bichurin

Citation: Journal of Applied Physics **119**, 203101 (2016); doi: 10.1063/1.4951717
View online: http://dx.doi.org/10.1063/1.4951717
View Table of Contents: http://scitation.aip.org/content/aip/journal/jap/119/20?ver=pdfcov
Published by the AIP Publishing

JOURNAL OF APPLIED PHYSICS **119**, 203101 (2016)

Controlling the Goos-Hänchen shift with external electric and magnetic fields in an electro-optic/magneto-electric heterostructure

Yu. S. Dadoenkova,[1,2,3] F. F. L. Bentivegna,[4] N. N. Dadoenkova,[2,3] R. V. Petrov,[1] I. L. Lyubchanskii,[3] and M. I. Bichurin[1]

[1]*Institute of Electronic and Information Systems, Novgorod State University, 173003 Veliky Novgorod, Russian Federation*
[2]*Ulyanovsk State University, 432017 Ulyanovsk, Russian Federation*
[3]*Donetsk Physical and Technical Institute of the National Academy of Sciences of Ukraine, 83114 Donetsk, Ukraine*
[4]*Lab-STICC (UMR 6285), CNRS, UBL, École Nationale d'Ingénieurs de Brest, 29238 Brest Cedex 3, France*

(Received 2 March 2016; accepted 8 May 2016; published online 24 May 2016)

We present a theoretical investigation of the Goos-Hänchen effect upon light reflection from a heterostructure consisting of an electro-optic film deposited on a magneto-electric film grown on a nonmagnetic dielectric substrate. It is shown that the linear magneto-electric interaction leads to an increase of the lateral shift even in the absence of any applied electric field. The presence of the electro-optic layer enables the control of the Goos-Hänchen shift and of the position of its maximum (with respect to the angle of incidence) through a variation of the magnitude and orientation of an applied electric field. It is also demonstrated that applying an external magnetic field in order to reverse the magnetization in the magnetic layer results (under the influence of the magneto-electric interaction in the system) in a sign reversal of the lateral shift but a nonreciprocal change of its amplitude. *Published by AIP Publishing.* [http://dx.doi.org/10.1063/1.4951717]

I. INTRODUCTION

When an optical beam with a finite spatial profile is reflected upon incidence on an optical system, the reflected beam may be laterally and angularly shifted with respect to the behavior predicted by geometric optics for idealized light rays. This phenomenon was observed for the first time in 1947 by Goos and Hänchen for linearly polarized light in a total internal reflection experiment.[1] Since then, similar effects were reported for arbitrary states of polarization and incidence angles[2] and for wave-like phenomena of various kinds, including acoustic waves (Shoch effect),[3] spin waves,[4] neutron beams,[5] or electron beams.[6] The Goos–Hänchen (GH) effect has found applications, for instance, in the design of an optical waveguide switch,[7] in the biosensing technologies (e.g., the measurement of E. Coli O157:H7 concentration[8]), or in the detection of chemical vapours.[9] In multilayered systems, the interference of waves propagating at slightly different angles and obeying Snell's law leads to an increase in the phase change between the incident and reflected beams, which results in giant GH shifts of the order of tens or even hundreds of light wavelengths.[10,11] Particularly, large GH shifts were predicted in the vicinity of the Brewster angle.[2,12] In magneto-optical materials, the GH shift can also typically reach values up to several tens of light wavelengths.[13–15] Thus, the GH shift ought to be taken into account for the design of integrated optical or magneto-optical devices, either in order to reduce it or in view of enhancing it. On the other hand, even small variations of the permittivity and permeability of the constituents of an optical system can exert a significant influence on the GH shift. Given that such variations can be due to any change in the environment of the system, a direct monitoring of the GH shift seems to be a promising way to design simple and stable phase-sensitive detection and sensor devices.[8]

A particular interest can be found in the investigation and exploitation of the GH lateral shift in complex structures including functional materials, i.e., materials possessing order parameters of various natures that can be controlled through an external source of electric or magnetic fields, temperature, intense electromagnetic radiation, etc., thus inducing a modification of their properties. For instance, a change of the GH shift for a circularly polarized Gaussian beam *via* the application of a pump field and a coherent driving field to an atomic medium was recently discussed,[16] as was the possibility of controlling the GH shift with temperature in superconducting multilayers.[11,12] Similarly, it has been reported that a modification of the GH shift in the near-infrared domain at a Ce-doped yttrium-iron garnet (YIG) film surface can be achieved by magnetizing the film along specific directions.[15] The lateral shift upon light reflection of far-infrared electromagnetic radiation close to the frequency of magnon resonance can also be nonreciprocally inverted by a reversal of the magnetic field in an antiferromagnet.[17] In the same manner, it can be efficiently tuned through the application of an electric field to an optical system including an electro-optic layer.[18,19] Consequently, a combination of materials exhibiting magneto-optic and electro-optic properties in a photonic system opens the wider possibility to control the GH shift *via* the application of both a magnetic and an electric fields.

It is a well-established fact that the reflection of light from a magnetic material in the optical and near-infrared domains is a powerful tool for the study of magnetic materials, surfaces, and interfaces.[20] It is also well-known that a specific class of magnetic materials possesses spontaneous magneto-electric (ME) properties.[21] The ME effect, which results in the induction of a magnetization by an electric field or that of a dielectric polarization by a magnetic field, was indeed observed in many systems, including Cr_2O_3,[22] Ti_2O_3,[23] $GaFeO_3$,[24] garnet films,[25,26] or multiferroic composite heterostructures.[27,28] As a rule, the ME effect is allowed in materials whose magnetic point groups do not allow time reversal and spatial inversion symmetries.[29] It has also been shown that the ME interaction modifies the complex reflectivity factor of a magnetic/dielectric bilayer,[30–32] which in turn governs the GH effect. It can thus be expected that the spontaneous magneto-electricity also affects the lateral shift of a light beam upon reflection from such a heterostructure.

The purpose of this paper is thus threefold: first, to investigate the influence of the linear ME interaction on the lateral and angular GH shifts experienced by a Gaussian light beam reflected from a multilayered system consisting of an ME slab grown on a nonmagnetic dielectric substrate; second, to study the possibility of controlling the GH shifts *via* an external electric field and of enhancing such a control through the addition of an electro-optic layer to the system; and third, to investigate the influence of a magnetization reversal on the GH effect in this structure. The paper is organized as follows. Section II presents the description of an analytical calculation of the GH shifts using the stationary phase method, as well as the constitutive material equations of each medium and the derivation of the reflection coefficients of the multilayered structure. In Section III, we show the results of our numerical calculations of both the spatial and the angular GH shifts in the case of an electro-optic/magneto-electric system and provide an analysis of their behavior with respect to the incidence angle of light, the initial magnetization orientation in the magnetic layer, and the direction and magnitude of an external electric field. In Section IV, we summarize the results of our simulations and draw the conclusions of our study.

II. GENERAL ANALYSIS

A. Description of the system

Let us consider the reflection of a monochromatic electromagnetic wave from a bilayer consisting of a non-magnetic electro-optic slab of thickness d_1 grown on a magnetic slab of thickness d_2. This anisotropic bilayer is deposited on a semi-infinite isotropic dielectric substrate, as illustrated in Fig. 1.

The interfaces between the materials are parallel to the (xy) plane of a Cartesian system of coordinates. An electromagnetic wave of wavelength λ_0 impinges on the vacuum upper surface under an oblique incidence angle θ. Without loss of generality, the plane of incidence can be chosen as (xz) and the incident and reflected waves can be decomposed into s- and p-components of their electric field strengths $E^{(i,r)}_{s,p}$ with respect to that plane, where superscripts (i) and (r) correspond to the incident and reflected components, respectively. The system can be subjected to an external, static electric field $\mathbf{E}^{(ex)}$ parallel to the interfaces, at an angle φ with the plane of incidence of the electromagnetic wave. The magnetic slab is initially magnetized at saturation in the polar magneto-optical configuration, i.e., along the z-axis, and its magnetization can be reversed *via* an externally applied magnetic field $\mathbf{H}^{(ex)}$. We assume that the magnetic medium is characterized by a linear ME interaction. A variation in the direction of the static electric field may thus modify the direction of magnetization in the magnetic layer and, as a consequence, the overall optical properties of the system. The presence of the nonmagnetic electro-optic layer on top of the system is meant to enhance the influence of the external electric field on these properties.

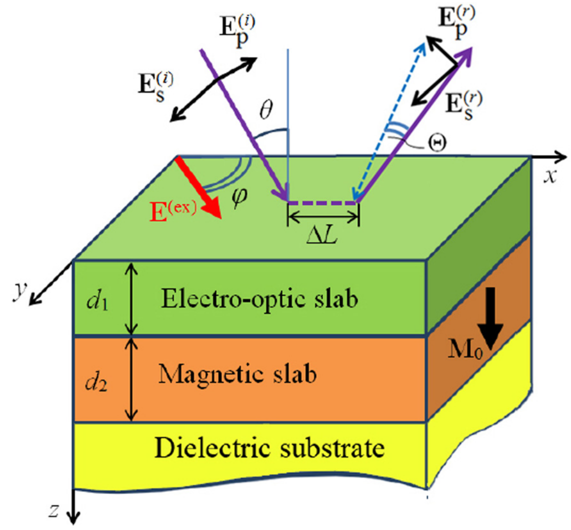

FIG. 1. Schematic of the system under study: an electro-optic slab (thickness d_1) on a magnetic slab (thickness d_2), grown on a semi-infinite isotropic dielectric substrate. The nominal saturation magnetization $\mathbf{M}_0 = \{0, 0, M_s\}$ in the magnetic slab is perpendicular to the planes of the slabs. The s- and p-components of the incident (i) and reflected (r) optical electric fields are denoted $E^{(i,r)}_{s,p}$. The spatial and angular GH shifts in the plane of incidence upon reflection are ΔL and Θ, respectively.

When a monochromatic Gaussian wavepacket of waist w_0 impinges on the uppermost surface of the thin film, its reflection is known to depart from the behavior predicted by ray optics, in which it undergoes a non-negligible GH lateral shift ΔL in the plane of incidence (in our case, along the x-axis), as well as an angular shift Θ in the same plane (Fig. 1). The values of the lateral and angular shifts can be obtained with the stationary-phase approach initially proposed by Artmann.[33] For any distribution of the x-component k_x of the incident wavevector, the lateral shift of the reflected wavepacket is deduced from the modulus $|R|$ and phase ψ of the complex reflectivity factor, with[14]

$$\Delta L = -\frac{\partial\psi}{\partial k_x} + \frac{\partial \ln|R|}{\partial k_x}\frac{\partial^2\psi}{\partial k_x^2}\left(w_0^2 + \frac{\partial^2 \ln|R|}{\partial k_x^2}\right)^{-1}, \quad (1)$$

while the angular shift can in first approximation be expressed as

$$\Theta = -\left(\theta_0^2/2\right)\frac{\partial\left(\ln|R|\right)}{\partial k_x}, \quad (2)$$

where the parameter $\theta_0 = \lambda_0/(\pi w_0)$ is the angular spread of the incident beam. The GH lateral shift ΔL is taken to be positive towards the positive direction of the x-axis, and the angular shift Θ is counted positive for a clockwise rotation with respect to the positive direction of the y-axis (in Fig. 1, both shifts are thus positive).

B. Constitutive relations and reflection coefficients

Phenomenologically, the ME effect in the magnetic medium manifests itself through a linear, reciprocal relationship between the magnetic field and the electric polarization and between the electric field and the magnetization.[29] The electro-optic effect in the non-magnetic medium, on the other hand, consists in a dependence of its optical properties on the external electric field.[35]

The electric displacement vector $\mathbf{D}^{(l)}$ and the magnetic induction $\mathbf{B}^{(l)}$ in each layer (l) of the system are, in the linear approximation, connected with the electric field $\mathbf{E}^{(l)}$ and the magnetic field $\mathbf{H}^{(l)}$ of the electromagnetic wave *via* constitutive material relations as follows:[34]

$$\begin{aligned} D_i^{(l)} &= \varepsilon_0 \varepsilon_{ij}^{(l)} E_j^{(l)}, \\ B_i^{(l)} &= \mu_0 H_j^{(l)}, \end{aligned} \tag{3}$$

in the electro-optic layer $(l=1)$ and dielectric substrate $(l=3)$, and[21]

$$\begin{aligned} D_i^{(2)} &= \varepsilon_0 \varepsilon_{ij}^{(2)} E_j^{(2)} + \alpha_{ij} H_j^{(2)}, \\ B_i^{(2)} &= \mu_0 \mu_{ij}^{(2)} H_j^{(2)} + \alpha_{ij} E_j^{(2)}, \end{aligned} \tag{4}$$

in the ME layer $(l=2)$. In Eqs. (3) and (4), ε_0 and μ_0 are the vacuum permittivity and permeability, $\varepsilon_{ij}^{(l)}$ and $\mu_{ij}^{(l)}$ are the relative permittivity and permeability tensor elements of the corresponding layer, and α_{ij} are the elements of the linear ME tensor of the magnetic film. In the optically isotropic dielectric substrate, $\varepsilon_{ij}^{(3)} = \tilde{\varepsilon}^{(3)} \delta_{ij}$, where δ_{ij} is the Kronecker symbol.

In the electro-optic medium with a cubic crystal symmetry, the inverse relative dielectric permittivity tensor can be represented as a power series of the static applied electric field components $E_k^{(\mathrm{ex})}$ $(k = x, y, z)$ as follows:[35]

$$(\varepsilon_{ij}^{(1)})^{-1} = (\tilde{\varepsilon}^{(1)})^{-1} \delta_{ij} + r_{ijk} E_k^{(\mathrm{ex})} + s_{ijkl} E_k^{(\mathrm{ex})} E_l^{(\mathrm{ex})} + \ldots, \tag{5}$$

where $\tilde{\varepsilon}^{(1)}$ is the isotropic relative permittivity in the absence of an externally applied electric field, and r_{ijk} and s_{ijkl} are the linear and quadratic electro-optic tensors of the medium, respectively. Higher-order terms in Eq. (10) can usually be neglected. Tensors r_{ijk} and s_{ijkl} possess the following permutation properties: $r_{ijk} = r_{jik}$, $s_{ijkl} = s_{jikl}$, and $s_{ijkl} = s_{jilk}$, and in cubic crystals they have the following nonzero components:[35] $r_{41} = r_{52} = r_{63}$, $s_{11} = s_{22} = s_{33}$, $s_{12} = s_{13} = s_{21} = s_{23} = s_{31} = s_{32}$, and $s_{44} = s_{55} = s_{66}$, where the usual reduced matrix symbols for the representation of higher-rank tensors are used, i.e., $1 \equiv 11$, $2 \equiv 22$, and $4 \equiv 23$.

Magnetic garnets, which are widely used in magnetophotonic devices, exhibit bigyrotropic properties in the near-infrared regime, i.e., their relative permittivity and permeability tensors both depend on the local magnetization. The numerical simulations described in Section III will be carried out with such a magnetic garnet as magnetic medium. Hence, tensors $\hat{\varepsilon}^{(2)}$ and $\hat{\mu}^{(2)}$ can be expanded in power series of the magnetization vector $\mathbf{M}$.[20] Neglecting terms above the first-order terms in such expansions, they write

$$\varepsilon_{ij}^{(2)} = \tilde{\varepsilon}^{(2)} \delta_{ij} + \delta\varepsilon_{ij}, \quad \mu_{ij}^{(2)} = \tilde{\mu}^{(2)} \delta_{ij} + \delta\mu_{ij}, \tag{6}$$

where $m_i = M_i/|\mathbf{M}|$, $\tilde{\varepsilon}^{(2)}$ and $\tilde{\mu}^{(2)}$ are the crystallographic components of the relative permittivity and permeability tensors of the medium, $\delta\varepsilon_{ij} = i f_{ijk}^{(e)} m_k$ and $\delta\mu_{ij} = i f_{ijk}^{(m)} m_k$ are the magnetically dependent contributions, and $f_{ijk}^{(e)}$ and $f_{ijk}^{(m)}$ are the linear (in magnetization) gyroelectric and gyromagnetic tensor elements of the crystal, respectively. For cubic crystals belonging to point symmetry groups T_d, O, and O_h, the latter reduces to scalars called the linear gyroelectric coefficient $f^{(e)}$ and linear gyromagnetic coefficient $f^{(m)}$ of the medium, respectively. Moreover, in such cubic crystals, the nonzero components of the magnetically induced contributions to tensors $\hat{\varepsilon}^{(2)}$ and $\hat{\mu}^{(2)}$ are

$$\begin{aligned} &\delta\varepsilon_{xy} = -\delta\varepsilon_{yx} = i f^{(e)} m_z, \quad \delta\mu_{xy} = -\delta\mu_{yx} = i f^{(m)} m_z, \\ &\delta\varepsilon_{xz} = -\delta\varepsilon_{zx} = -i f^{(e)} m_y, \quad \delta\mu_{xz} = -\delta\mu_{zx} = -i f^{(m)} m_y, \\ &\delta\varepsilon_{yz} = -\delta\varepsilon_{zy} = i f^{(e)} m_x, \quad \delta\mu_{yz} = -\delta\mu_{zy} = i f^{(m)} m_x. \end{aligned} \tag{7}$$

The impact of the ME effect on the magnetization can be deduced from the expression of the free energy F of the magnetic medium written in terms of the external static magnetic and electric fields $\mathbf{H}^{(\mathrm{ex})}$ and $\mathbf{E}^{(\mathrm{ex})}$ to which it is subjected as[29]

$$\begin{aligned} -F\left(E^{(\mathrm{ex})}, H^{(\mathrm{ex})}\right) = \frac{1}{2}\varepsilon_0 \varepsilon_{ij} E_i^{(\mathrm{ex})} E_j^{(\mathrm{ex})} + \frac{1}{2}\mu_0 \mu_{ij} H_i^{(\mathrm{ex})} H_j^{(\mathrm{ex})} \\ + \alpha_{ij} E_i^{(\mathrm{ex})} H_j^{(\mathrm{ex})} + \ldots. \end{aligned} \tag{8}$$

For any set of externally applied fields and experimental conditions, equilibrium in the medium is reached when its free energy is minimal. The first and second terms on the right-hand side of Eq. (8) describe the electric and magnetic responses of the system to an electric and a magnetic fields, respectively. The third term describes the linear ME coupling *via* the ME tensor $\hat{\alpha}$, which is diagonal $(\alpha_{ij} = \alpha\, \delta_{ij})$ in crystals with a cubic symmetry.[36] The ME contribution to the magnetization vector $\mathbf{M}$ is obtained by differentiating the free energy with respect to $H_i^{(\mathrm{ex})}$ and then setting $H_i^{(\mathrm{ex})} = 0$, so that $\mu_0 M_i = \alpha_{ij} E_j^{(\mathrm{ex})}$. In the absence of an ME interaction, the magnetic film is nominally magnetized to saturation along the z-axis (Fig. 1), with $\mathbf{M}_0 = M_s \hat{z}$. An externally applied electric field can only induce a precession of the magnetization vector around the z-axis while keeping its amplitude unchanged. In the presence of ME coupling, assuming that the external electric field $\mathbf{E}^{(\mathrm{ex})}$ is applied in the (xy)-plane, the components of the magnetization vector are written as

$$\begin{aligned} \mu_0 M_x &= \alpha E_x^{(\mathrm{ex})} \cos\varphi, \\ \mu_0 M_y &= \alpha E_y^{(\mathrm{ex})} \sin\varphi, \\ \mu_0 M_z &= \sqrt{\mu_0^2 M_s^2 - \alpha^2 |E^{(\mathrm{ex})}|^2}, \end{aligned} \tag{9}$$

where φ is the angle between the electric field and the x-axis (Fig. 1).

Note that in the absence of an external electric field, i.e., when the magnetization vector is along the z-axis (thus $m_x = m_y = 0$), the number of non-zero magnetically induced components of the permittivity and permeability tensors in Eq. (7) reduces, namely, $\delta\varepsilon_{xz} = \delta\varepsilon_{zx} = \delta\varepsilon_{yz} = \delta\varepsilon_{zy} = 0$ and $\delta\mu_{xz} = \delta\mu_{zx} = \delta\mu_{yz} = \delta\mu_{zy} = 0$. In the general case of an arbitrary orientation of the external electric field applied to the magnetic slab in the (xy)-plane, all components of the permittivity and permeability tensors are affected by the ME interaction.

Taking into account the boundary conditions at each interface of the system, one can then relate the amplitudes of the reflected $E_{s,p}^{(r)}$ and incident $E_{s,p}^{(i)}$ light field components as

$$\begin{pmatrix} E_s^{(r)} \\ E_p^{(r)} \end{pmatrix} = \hat{\Re} \begin{pmatrix} E_s^{(i)} \\ E_p^{(i)} \end{pmatrix}, \quad \text{with } \hat{\Re} = \begin{pmatrix} \Re_{ss} & \Re_{sp} \\ \Re_{ps} & \Re_{pp} \end{pmatrix}. \qquad (10)$$

In general, the reflection matrix $\hat{\Re}$ has four non-zero components. Its off-diagonal components correspond to cross-polarization upon reflection of light and arise from the combination of magneto-optic, ME, and electro-optic interactions in the anisotropic system. All four of the components depend in an intricate but analytical manner on the various material parameters and tensor components introduced above, as well as on the amplitude and direction of the externally applied electric and magnetic fields.

Using Eq. (10) and taking into account Eqs. (1) and (2), one can finally obtain the value of the GH lateral and angular shifts for each component of the reflected field. In Section III, these lateral shifts will be presented in the reduced form $\Delta X_{ij} = \Delta L_{ij}/\lambda_0$ (i, $j = s$, p). The reduced shift ΔX_{ps} (resp., ΔX_{sp}) thus describes the cross-polarized contribution to the GH effect, i.e., the lateral shift of a s- (resp., p-) polarized incident wave reflected into a p- (resp., s-) polarized wave.

III. RESULTS AND DISCUSSION

In this section, we present the results of numerical calculations of the GH shift performed in the case of an electro-optic slab of zinc selenide ZnSe and a magnetic layer of yttrium iron garnet (YIG) $Y_3Fe_50_{12}$ grown on a substrate of gadolinium gallium garnet (GGG) $Gd_3Ga_50_{12}$. It should be noted that in bulk YIG, the linear ME effect cannot be observed, since symmetry rules forbid it in crystals with an inversion center. However, in thin epitaxial films, symmetry lowering takes place and the inversion center vanishes.[25,26] It has been demonstrated experimentally that the linear ME constant in thin (of about several microns thickness) YIG films can reach large values up to 30 ps m^{-1}.[25,26]

The characteristics of the light beam, the dimensions of the structure, and the material parameters used for these simulations are collected in Table I.

As follows from Eqs. (1) and (2), the spatial and angular GH shifts are described in terms of the complex reflection coefficient R of an incident light beam. This coefficient depends on the material parameters of all the constitutive layers of the structure (gathered in Table I) as well as on the

TABLE I. Physical data used for calculations.

Light beam wavelength	$\lambda_0 = 1.15\ \mu$m
Gaussian beam waist	$w_0 = 100\ \mu$m
Thicknesses of the slabs	$d_1 = 2\ \mu$m, $d_2 = 2\ \mu$m
ZnSe relative permittivity tensor elements (at λ_0)[37]	$\tilde{\varepsilon}^{(1)} = 6.1254$
ZnSe electro-optic constants[35]	$r_{14} = 2 \times 10^{-12}$ m V^{-1}; $s_{11} = s_{12} = s_{44} \sim 10^{-18}$ m^2 V^{-2}
YIG saturation magnetization[38]	$M_s = 143$ kA m^{-1}
YIG relative permittivity tensor elements (at λ_0)[39]	$\tilde{\varepsilon}^{(2)} = 4.5796, f^{(e)} = -2.47 \times 10^{-4}$
YIG relative permeability tensor elements (at λ_0)[39]	$\tilde{\mu}^{(2)} = 1, f^{(m)} = 8.75 \times 10^{-5}$
YIG magneto-electric constant[26]	$\alpha = 30$ ps m^{-1}
GGG relative permittivity (at λ_0)[39]	$\tilde{\varepsilon}^{(3)} = 3.7636$

wavelength λ_0 and incidence angle θ of the incoming light beam. Thus, any modification of the aforementioned parameters following the application of an electric or a magnetic field is likely, in turn, to affect the GH lateral and angular shift of light upon reflection. Of all parameters, the applied static electric field $\mathbf{E}^{(ex)}$ plays the most versatile role, as it modifies the permittivity of the electro-optic layer [Eq. (5)] and alters the direction of the magnetization vector in the magnetic layer *via* the ME effect [Eqs. (8) and (9)] and thus the permittivity and permeability tensors of that layer through their magnetization-dependent components.

In the following, the influence on the GH effect of the applied electric field, of the presence of an electro-optic top layer, and of the ME effect in the magnetic layer is discussed.

A. Goos-Hänchen shift without externally applied fields

The presence of the electro-optic layer on top of the magnetic slab is one of the parameters that bears an effect on the optical response of the system. Figure 2 thus addresses the role of the ZnSe electro-optic layer in the lateral GH shift when no static electric field is applied, but the ME effect is nevertheless taken into account in the magnetic YIG film. Specifically, the dependence of the reduced shifts ΔX_{ij} upon the incidence angle θ of the incoming light beam in the YIG/GGG system, i.e., without electro-optic layer [Fig. 2(a)], is compared with the same dependence in the ZnSe/YIG/GGG heterostructure [Fig. 2(b)]. Due to the symmetry properties of the materials, the cross-polarized contributions to the GH shift are equal ($\Delta X_{ps} = \Delta X_{sp}$) and will henceforth be denoted ΔX_{ps}.

The results show that ΔX_{ss} (lateral shift observed upon the reflection of a s-polarized incident wave into a similarly s-polarized wave) remains negligible (less than one wavelength λ_0), with or without electro-optic layer, while ΔX_{pp} (lateral shift upon the reflection of a p-polarized incident wave into a similarly p-polarized wave) and particularly the cross-polarized contribution ΔX_{ps} can reach values up to several wavelengths at the incidence angles θ around 60° and 75°, respectively, in the YIG/GGG system [Fig. 2(a)]. At grazing incidence, ΔX_{pp} reverses sign and the shift is

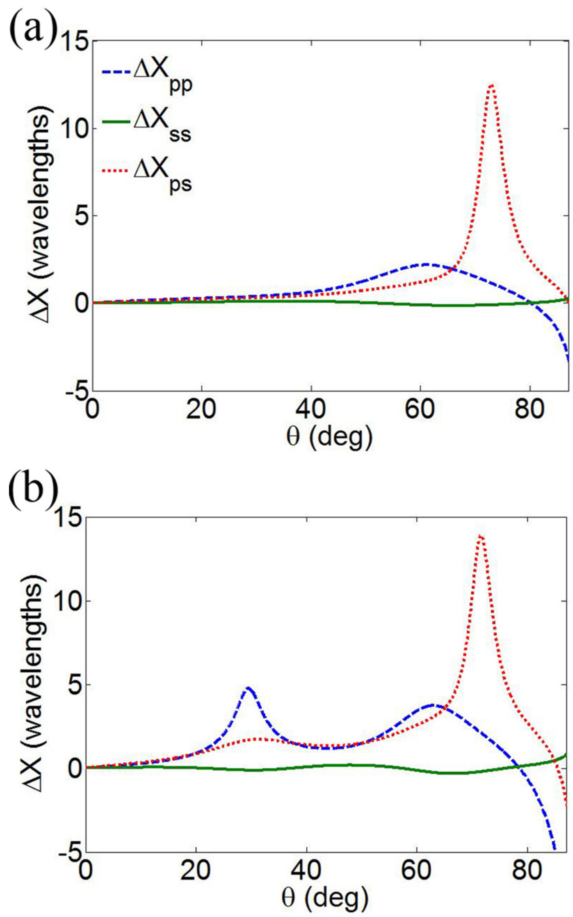

FIG. 2. Reduced lateral shifts ΔX_{pp} (dashed blue line), ΔX_{ss} (solid green line), and $\Delta X_{ps} = \Delta X_{sp}$ (dotted red line) as functions of the incidence angle θ without external electric field: (a) in the YIG/GGG structure and (b) in the ZnSe/YIG/GGG structure. The ME interaction is taken into account.

directed towards negative values of the x-axis. The introduction of an electro-optic slab results in a slight increase of ΔX_{ps} around 75°, and in the formation of a second maximum of ΔX_{ps} and especially ΔX_{pp} at $\theta \approx 30°$. It should be noted that the maxima of ΔX_{ps} correspond to minimal values of the reflection coefficient R_{ps}. The lateral shift ΔX_{pp} does not exceed 2.5 λ_0 in the system without electro-optic layer, and twice that value in the presence of a ZnSe film. The largest lateral shifts (between 10 λ_0 and 15 λ_0) occur for the cross-polarized contribution ΔX_{ps}.

Further simulations show that applying a static electric field to the structures, with or without ZnSe electro-optic layer, has almost no effect on the values of the GH shifts ΔX_{pp} and ΔX_{ss}, at least for field magnitudes up to $E^{(ex)} = 10$ MV m^{-1}, where quadratic ME interactions may arise. On the contrary, the cross-polarized contribution to the lateral shift exhibits a strong electric-field dependence. Thus, further analyses will be devoted only to the various dependences of the cross-polarized contribution ΔX_{ps} to the lateral shift, but always in the presence of an external electric field.

B. Dependence of the Goos-Hänchen shift upon an externally applied electric field

Figure 3 first addresses the variations of the reduced lateral shift ΔX_{ps} in the YIG/GGG bilayer as a function of both the incidence angle θ of incoming light and the orientation angle ϕ of the external electric field, when the ME coupling is taken into account in the simulations [Fig. 3(a)] and when it is ignored, i.e., with $\alpha = 0$ [inset in Fig. 3(a)]. The latter case purports to evaluate the influence of that coupling on the GH shift. In both cases, the magnitude of the external electric field is $E^{(ex)} = 5$ MV m^{-1}.

Comparing Figs. 2(a) and 3(a) shows that in the absence of an electro-optic slab on top of the structure, the effect of the external electric field on the GH shift is negligible. The amplitude of the maximal shift around $\theta \approx 75°$ is virtually not affected by the application of the electric field, and the direction of that field bears no influence on the result—indeed, the evolution of ΔX_{ps} in Fig. 2(a) replicates any cross-section of the profile in Fig. 3(a), whatever the orientation angle φ of the applied electric field. The reason is that the off-diagonal components of the ε and μ tensors of the magnetic YIG, which depend on magnetization and are, through the ME coupling, sensitive to the applied electric field, appear to be too small to yield an efficient change to the corresponding reflection coefficient, and thus to the GH shift. Indeed, on the basis of Eq. (3) and the numerical data from Table I, the maximal value of the additional magnetization induced *via* the ME coupling by an electric field $\mathbf{E}^{(ex)}$ of magnitude 5 MV m^{-1} applied, for example, along the y-axis, is $M_y \approx 120$ A m^{-1}, which is 8.4% of the nominal saturation magnetization M_S along the z-axis. The magneto-electrically induced off-diagonal tensor components in this case [see Eq. (7)] are $\varepsilon_{xz} = -2.96 \times 10^{-6}$ and $\mu_{xz} = 1.05 \times 10^{-6}$, which are about two orders of magnitude less than the magnetization-induced off-diagonal components ε_{xy} and μ_{xy} of the permittivity and permeability tensors.

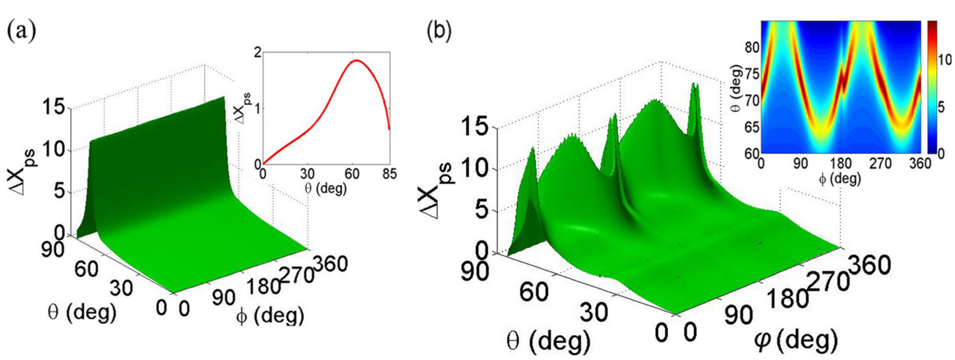

FIG. 3. Evolution of the reduced lateral shift ΔX_{ps} with the incidence angle θ and the orientation angle φ of the external electric field in the (a) YIG/GGG structure and (b) ZnSe/YIG/GGG structure, when the ME effect is taken into account. The inset in (a) shows ΔX_{ps} if the effect of the ME coupling is ignored. The inset in (b) presents a color map of ΔX_{ps} in the vicinity of its maximal values. The magnitude of the external electric field is $E^{(ex)} = 5$ MV m^{-1} in all cases.

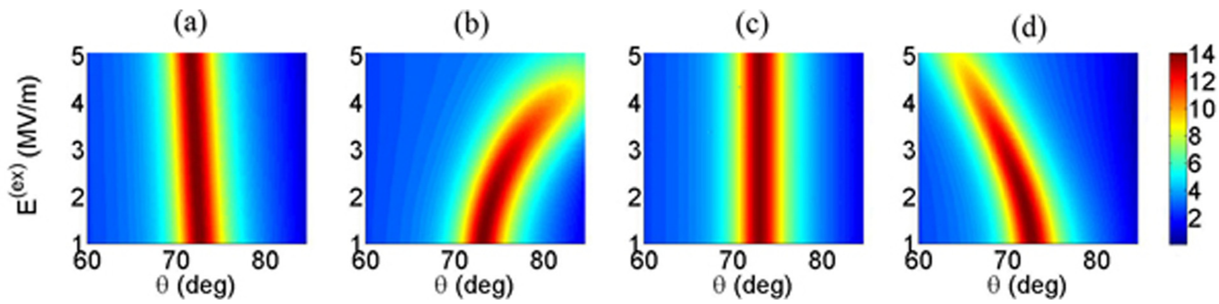

FIG. 4. Color maps showing the evolution of the reduced lateral shift ΔX_{ps} with the incidence angle θ and the magnitude $E^{(ex)}$ of the external electric field in the ZnSe/YIG/GGG structure for different orientation angles of $\mathbf{E}^{(ex)}$: (a) $\varphi = 0°$; (b) $\varphi = 45°$; (c) $\varphi = 90°$; and (d) $\varphi = 135°$. The color scale shows the values of ΔX_{ps} in units of incident light wavelength λ_0.

Nevertheless, as a comparison of Fig. 3(a) and its inset, readily shows the ME interaction in the system, through its contribution to the constitutive equations describing the optical response of the magnetic medium [Eq. (3)], is strong even in the absence of any applied electric field and leads to an about sixfold increase of the GH shift ΔX_{ps} in the vicinity of $\theta \approx 75°$. The ME interaction manifests itself by modifying, through its contribution to the wavevectors of the light beams in the magnetic medium, the conditions for constructive or destructive interferences of counter-propagating waves in the structure. This effect is further enhanced when an electric field is applied to the system. Thus, in all further calculations, the ME interaction will be taken into account.

An enhancement of the influence of an applied electric field on the GH shift can, however, be expected through the inclusion of an electro-optic ZnSe top layer. Calculations similar to those displayed in Fig. 3(a) are thus now performed for a ZnSe/YIG/GGG heterostructure [Fig. 3(b)]. The profile of the GH shift ΔX_{ps} is now clearly dependent on the direction of the applied electric field $\mathbf{E}^{(ex)}$. The introduction of the ZnSe slab leads to a displacement of the angular position (in terms of the incidence angle θ of light) of the maximum of the GH shift, and this displacement itself varies with the orientation φ of the external field [see inset in Fig. 3(b)]. For example, for $\mathbf{E}^{(ex)}$ oriented within the [90°–180°] and [270°–360°] ranges with respect to the x-axis, the maximum of ΔX_{ps} drifts towards smaller incidence angles down to $\theta \approx 60°$, while for the electric field applied within the [0°–90°] and [180°–270°] ranges this maximum moves towards larger values of θ, up to grazing incidence.

In addition to the direction of the applied electric field, its magnitude is bound to play a role, particularly when an electro-optic layer enhances its effect, in the control of the GH shift. As a complement to Fig. 3, the dependence of ΔX_{ps} upon the angle of incidence of the incoming wave and the magnitude $E^{(ex)}$ of the electric field is represented in Fig. 4 for several orientations φ of $\mathbf{E}^{(ex)}$ and a field magnitude varying between 1 and 5 MV m^{-1}. The range of variation for the angle of incidence θ is limited to the vicinity of the main maximum of ΔX_{ps}. Our calculations show that neither the amplitude nor the position of the maximum of ΔX_{ps} depends on the electric field amplitude when that field is applied perpendicular to the plane of incidence of light [$\varphi = 90°$, Fig. 4(c)], while only the position of that maximum very slightly shifts towards lower values of θ for an increasing field applied along the plane of incidence [$\varphi = 0°$, Fig. 4(a)]. For an electric field applied along an intermediary direction, both the amplitude and the position of the maximum of ΔX_{ps} vary with the magnitude $E^{(ex)}$ of the electric field. As could be seen in Fig. 3(b), the amplitude of the maximal cross-polarized GH shift decreases when the field increases, and its position clearly drifts towards larger [$\varphi = 45°$, Fig. 4(b)] or smaller [$\varphi = 135°$, Fig. 4(d)] values of the incidence angle. Overall, one notices an asymmetry of the response that can be attributed to the asymmetry of the linear and quadratic electro-optic effects with respect to the direction of $\mathbf{E}^{(ex)}$ [see Eq. (10) and the symmetries of the r_{ijk} and s_{ijkl} tensors].

C. Dependence of the Goos-Hänchen shift upon magnetization-reversal

Yet, another parameter allowing some measure of control of the GH shift in the system under study is the magnetization of the YIG magnetic layer. All the previous calculations were

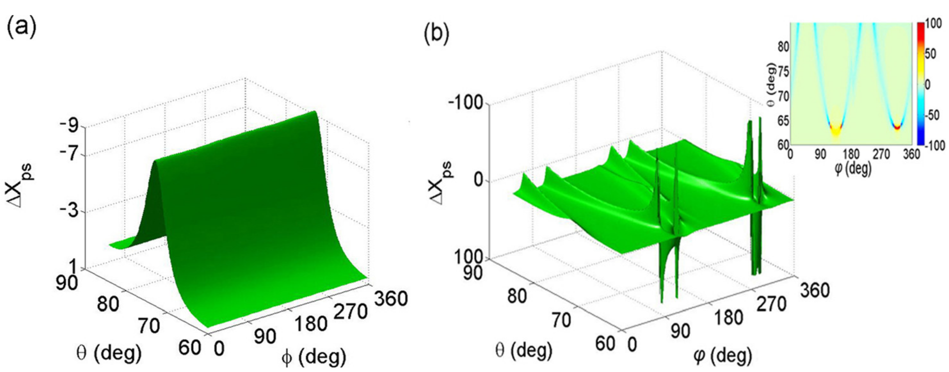

FIG. 5. Evolution of the reduced lateral shift ΔX_{ps} with the incidence angle θ and the orientation angle ϕ of the external electric field in the (a) YIG/GGG structure and (b) in ZnSe/YIG/GGG structure upon a reversal of the magnetization. The inset in (b) presents a color map of ΔX_{ps} in the vicinity of its maximal values. The magnitude of the external electric field is $E^{(ex)} = 5$ MV m^{-1}. Note the reversal of the vertical scale.

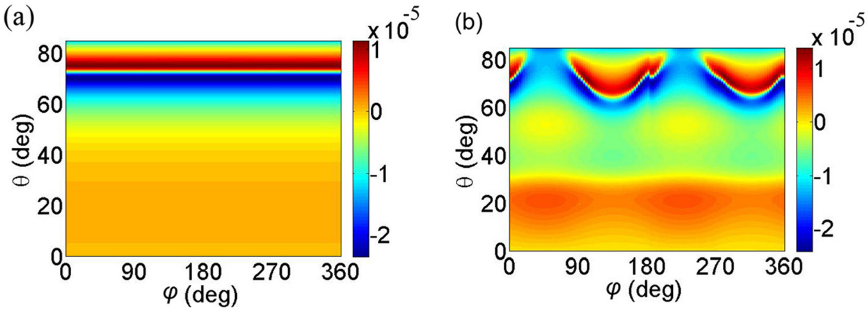

FIG. 6. Evolution of the cross-polarized angular GH shift Θ_{ps} with the incidence angle of light θ and the orientation angle ϕ of the external electric field in (a) YIG/GGG structure and (b) ZnSe/YIG/GGG structure. The magnitude of the external electric field is $E^{(ex)} = 5$ MV m^{-1}. The ME interaction is taken into account. The color scale shows the values of Θ_{ps} in radians.

performed with a magnetic layer magnetized to saturation along the positive direction of the z-axis. Figure 5(a) illustrates the effect of a magnetization reversal, imposed by the externally applied static magnetic field $\mathbf{H}^{(ex)}$, in the same system (YIG/GGG bilayer) and under the same conditions (other than the magnetization direction) as in Fig. 3(a). The nominal magnetization in the YIG layer is thus $\mathbf{M}_0 = -M_s\hat{\mathbf{z}}$. Comparing Figs. 5(a) and 3(a) shows a remarkable nonreciprocity of the GH effect upon magnetization reversal. As in Fig. 3(a), the influence of the applied electric field is negligible, and for the same reason (the absence of an electro-optic layer that enhances that influence), so that ΔX_{ps} does not vary with φ. The profile of ΔX_{ps} as a function of the angle of incidence θ does not exhibit a symmetrical behaviour in comparison to its counterpart of Fig. 3(a): the peak around the maximum of $|\Delta X_{ps}|$ is less sharp, and the values taken by ΔX_{ps} are not simply the opposite of those obtained for $\mathbf{M}_0 = +M_s\hat{z}$, and they reach smaller values as a whole. Furthermore, additional calculations show that in the absence of ME interaction, a magnetization reversal from $\mathbf{M}_0 = +M_s\hat{z}$ to $\mathbf{M}_0 = -M_s\hat{z}$ does not induce a sign change of the GH shift and induces a variation of ΔX_{ps} that does not exceed about 0.1 λ_0. This means that the ME effect plays an essential part in the behavior of the GH shift upon magnetization reversal. In essence, the nonreciprocal change of profile of ΔX_{ps} can be attributed to the interaction between the magneto-optic and the ME couplings in the bilayer.

Figure 5(b) illustrates the effect of a magnetization reversal in the ZnSe/YIG/GGG trilayer, under the same conditions (other than the magnetization direction) as in Fig. 3(b). The profile of the cross-polarized GH shift ΔX_{ps} in Fig. 5(b) now differs greatly from that shown in Fig. 5(a) (without ZnSe layer). A comparison of Figs. 3(b) and 5(b), however, demonstrates again an obviously nonreciprocal behavior of ΔX_{ps} upon magnetization reversal, as can be seen near grazing incidence. Moreover, when the orientation angle φ of the external electric field lies within the ranges [110°–150°] and [310°–340°], ΔX_{ps} can reach very high values, up to about 100 λ_0 in both positive and negative directions. The corresponding narrow peaks of cross-polarized GH shifts observed in Fig. 5(b) at incidence angles around 60° were not present for a magnetization of the YIG layer in the positive direction of the z-axis. However, further analysis shows that these huge values of ΔX_{ps} coincide with almost zero reflectivity, which would make it difficult to detect them in practice. It should also be noted that the lateral shift exhibits an additional asymmetry upon magnetization reversal, which appears, for instance, when comparing its values around $\varphi = 135°$ and $\varphi = 315°$ [see inset in Fig. 5(b)]. Such asymmetry is less pronounced for $\mathbf{M}_0 = +M_s\hat{z}$, as the inset in Fig. 3(b) demonstrates.

D. Angular Goos-Hänchen shift

Finally, keeping in mind that the lateral GH shift is in any case coupled to an angular counterpart Θ in the plane of incidence [see Fig. 1 and Eq. (6)], we briefly investigate the behavior of the angular shift. Similar to what was noticed for the spatial lateral shifts ΔX_{pp} and ΔX_{ss}, the corresponding angular shifts Θ_{pp} and Θ_{ss} show no pronounced dependence on the external electric field, whereas our calculations show that the cross-polarized angular shift Θ_{ps} does (note that for reasons of symmetry identical to those previously invoked, the cross-polarized contributions to the angular GH shift are equal, i.e., $\Theta_{sp} = \Theta_{ps}$). In Figs. 6(a) and 6(b), the variation of the cross-polarized angular shift Θ_{ps} with the incidence angle θ and the orientation angle φ of the external electric field is shown for the YIG/GGG and ZnSe/YIG/GGG systems, respectively. Here, the YIG magnetic layer is magnetized to saturation with $\mathbf{M}_0 = +M_s\hat{z}$, the magnitude of the applied electric field is $E^{(ex)} = 5$ MV m^{-1}, and the ME interaction is taken into account.

As earlier, we estimated the effect of the ME interaction by comparing the results shown in Fig. 6 with those obtained when it is neglected (with $\alpha = 0$) and concluded that the angular shift in that approximation is at least one order of magnitude less than when the ME coupling is indeed accounted for. However, it appears from the results displayed in Fig. 6 that even then, the maximal value of Θ_{ps} does not exceed 2.5×10^{-5} rad in absolute value. Like Fig. 3(a) for the lateral shift, and for the same reasons, Fig. 6(a) shows that in the absence of a ZnSe electro-optic layer on top of the structure, the effect of the external electric field on the GH shift is negligible, and the profile of Θ_{ps} does not vary with the direction of that field. And like Fig. 3(b) for ΔX_{ps}, Fig. 6(b) demonstrates that Θ_{ps} does exhibit a strong dependence upon the direction of $\mathbf{E}^{(ex)}$ when an electro-optic layer is introduced, which enhances the influence of that field. The drift of the extrema of the angular shift observed around $\theta \approx 75°$ in the ZnSe/YIG/GGG structure when the direction of $\mathbf{E}^{(ex)}$ varies is very similar to that demonstrated in Fig. 3(b) for the lateral shift. The positions of these extrema reproduce those observed for ΔX_{ps}.

IV. CONCLUSION

In this paper, we have proposed a detailed theoretical investigation of the Goos-Hänchen effect upon light reflection from a three-constituent magneto-electric heterostructure consisting of an electro-optic slab of ZnSe deposited on a thin epitaxial film magnetic yttrium-iron garnet, itself grown on a thick nonmagnetic dielectric substrate of gadolinium-gallium garnet. External, static magnetic and electric fields can be applied to the structure, and the presence of the electro-optic layer is meant to enhance the effect of the electric field on the Goos-Hänchen shift.

Our results show that the linear magneto-electric interaction in the magnetic slab leads to an about sixfold increase of the cross-polarized contribution to the lateral shift (i.e., a lateral shift of a *s*- (*p*-) polarized reflected wave originating in a *p*- (*s*-) polarized incident wave) even in the absence of any applied electric field and in the absence of the electro-optic layer, whereas the lateral shift of a *s*- (*p*-) polarized incident wave reflected into a *s*- (*p*-) polarized wave does not show any noticeable change related to either the magneto-electric coupling or the external electric field. However, we show that the magneto-electric interaction alone is not strong enough to provide non-negligible changes to the cross-polarized contribution to the lateral shift when the external electric field is applied to the system without electro-optic film. The latter, when present, does exert a strong influence, enhancing the effect of the electric field on the properties of the reflected light.

Both the spatial and the angular Goos-Hänchen shifts can be controlled through a variation of the direction and the magnitude of the external electric field. In particular, the amplitude of the maximal cross-polarized Goos-Hänchen shift decreases when the magnitude of the applied electric field increases, and its angular position (in terms of incidence angle) can itself be shifted when the electric field is neither parallel to the plane of incidence of light ($\varphi = 0$) nor perpendicular to it ($\varphi = \pi/2$).

On the other hand, inverting the direction of the external magnetic field, and thus reversing the initial magnetization of the magnetic film, results in a non-symmetrical inversion of the Goos-Hänchen shift, i.e., a sign reversal of the shift but a nonreciprocal change of its amplitude. Neglecting the magneto-electric interaction in the magnetic layer in the calculations, however, does not lead to inversion of the lateral shift, which means that the magneto-electric effect plays an essential part in the behavior of the Goos-Hänchen shift upon magnetization reversal. More generally, the nonreciprocal inversion of the lateral shift can be attributed to a complex interplay between the magneto-optic and magneto-electric couplings in the bilayer.

As our results show, a well-chosen combination of applied electric and magnetic fields (amplitude and direction) makes it possible to use this interplay in order to efficiently control, enhance, or reduce the Goos-Hänchen shift in the magneto-electric heterostructure investigated in this paper. As a consequence, the use of magneto-electric materials in a photonic structure can be expected to find applications, through the measurement of the Goos-Hänchen shift they induce, for instance, to the determination of very tiny variations of material properties or to the design of magnetically tunable optical switches and sensors.

ACKNOWLEDGMENTS

This research was supported partly by a grant (Project No. 15-19-10036) from the Russian Science Foundation (Yu.S.D., R.V.P., and M.I.B.) and a grant (Project No. 14.Z50.31.0015) from the Ministry of Education and Science of the Russian Federation (Yu.S.D. and N.N.D.). It was also partly supported by the European Union's Horizon 2020 research and innovation programme under the Marie Skłodowska-Curie Grant Agreement No. 644348 "MagIC," by the MPNS COST Action MP1403 "Nanoscale Quantum Optics," and by the Grant No. 14MOESMOMO14 of ENIB (Yu.S.D., N.N.D., and I.L.L.).

[1]F. Goos and H. Hänchen, Ann. Phys. **436**, 333–346 (1947).
[2]K. Y. Bliokh and A. Aiello, J. Opt. **15**, 014001 (2013).
[3]N. F. Declercq and E. Lamkanfi, Appl. Phys. Lett. **93**, 054103 (2008).
[4]P. Gruszecki, J. Romero-Vivas, Yu. S. Dadoenkova, N. N. Dadoenkova, I. L. Lyubchanskii, and M. Krawczyk, Appl. Phys. Lett. **105**, 242406 (2014).
[5]X. Chen, X. J. Lu, Y. Ban, and C. F. Li, J. Opt. **15**, 033001 (2013).
[6]V.-O. de Haan, J. Plomp, T. M. Rekveldt, W. H. Kraan, A. A. van Well, R. M. Dalgliesh, and S. Langridge, Phys. Rev. Lett. **104**, 010401 (2010).
[7]T. Sakata, H. Togo, and F. Shimokawa, Appl. Phys. Lett. **76**, 2841–2843 (2000).
[8]J. Sun, X. Wang, C. Yin, P. Xiao, H. Li, and Z. Cao, J. Appl. Phys. **112**, 083104 (2012).
[9]Y. Nie, Y. Li, Z. Wu, X. Wang, W. Yuan, and M. Sang, Opt. Express **22**, 8943–8948 (2014).
[10]I. V. Soboleva, V. V. Moskalenko, and A. A. Fedyanin, Phys. Rev. Lett. **108**, 123901 (2012).
[11]Yu. S. Dadoenkova, N. N. Dadoenkova, I. L. Lyubchanskii, Y.-P. Lee, and Th. Rasing, Photonics Nanostruct.: Fundam. Appl. **11**, 345–352 (2013).
[12]Yu. S. Dadoenkova, N. N. Dadoenkova, I. L. Lyubchanskii, and Y. P. Lee, J. Appl. Phys. **118**, 213101 (2015).
[13]S. B. Borisov, N. N. Dadoenkova, I. L. Lyubchanskii, and M. I. Lyubchanskii, Opt. Spectrosc. **85**, 225–231 (1998).
[14]Yu. S. Dadoenkova, F. F. L. Bentivegna, N. N. Dadoenkova, I. L. Lyubchanskii, and Y. P. Lee, J. Opt. Soc. Am. B **33**, 393–404 (2016).
[15]T. Tang, J. Qin, J. Xie, L. Deng, and L. Bi, Opt. Express **22**, 27042–27055 (2014).
[16]S. Asiri, J. Xu, M. Al-Amri, and M. Suhail Zubairy, Phys. Rev. A **93**, 013821 (2016).
[17]F. Lima, T. Dumelow, E. L. Albuquerque, and J. A. P. da Costa, J. Opt. Soc. Am. B **28**, 306–313 (2011).
[18]X. Wang, C. Yin, J. Sun, J. Gao, M. Huang, and Z. Cao, J. Opt. **15**, 014007 (2013).
[19]N. Goswami, A. Kar, and A. Saha, Opt. Commun. **330**, 169–174 (2014).
[20]A. K. Zvezdin and V. A. Kotov, *Modern Magnetooptics and Magnetooptical Materials* (Institute of Physics Publishing, Bristol, 1997).
[21]T. H. O'Dell, *The Electrodynamics of Magnetoelectric Media* (North-Holland, Amsterdam, 1970).
[22]I. E. Dzyaloshinskii, Sov. Phys.-JETP **10**, 628 (1959).
[23]B. I. Al'shin and D. N. Astrov, Sov. Phys.-JETP **17**, 809 (1963).
[24]G. T. Rado, Phys. Rev. Lett. **13**, 335 (1964).
[25]B. B. Krichevtsov, V. V. Pavlov, and R. V. Pisarev, JETP Lett. **49**, 535–539 (1989).
[26]B. B. Krichevtsov, V. V. Pavlov, R. V. Pisarev, and A. G. Selitsky, Ferroelectrics **161**, 65–71 (1994).
[27]M. Bichurin and V. Petrov, *Modeling of Magnetoelectric Effects in Composites* (Springer, London, 2014).
[28]C.-W. Nan, M. I. Bichurin, Sh. Dongb, D. Viehland, and G. Srinivasan, J. Appl. Phys. **103**, 031101 (2008).

[29]M. Fiebig, J. Phys. D: Appl. Phys. **38**, R123–R152 (2005).
[30]Yu. S. Dadoenkova, I. L. Lyubchanskii, Y. P. Lee, and Th. Rasing, Eur. Phys. J. B **71**, 401–406 (2009).
[31]Yu. S. Dadoenkova, I. L. Lyubchanskii, Y. P. Lee, and Th. Rasing, Low Temp. Phys. **36**, 538 (2010).
[32]Yu. S. Dadoenkova, I. L. Lyubchanskii, Y. P. Lee, and Th. Rasing, J. Opt. Soc. Am. B **31**, 626–630 (2014).
[33]K. Artmann, Ann. Phys. **437**, 87 (1948).
[34]M. Born and E. Wolf, *Principles of Optics* (Pergamon, London, 1997).
[35]A. Yariv and P. Yeh, *Optical Waves in Crystals* (Wiley, New York, 1984).
[36]R. R. Birss, *Symmetry and Magnetism* (North-Holland, Amsterdam, 1966).
[37]E. D. Palik, *Handbook of Optical Constants in Solids* (Academic Press, New York, 1991).
[38]*Landolt-Börnstein - Group III, Condensed Matter*, Magnetic and Other Properties of Oxides and Related Compounds - Part A: Garnets and Perovskites Vol. 12a, edited by K.-H. Hellwege and A. M. Hellwege (Springer-Verlag, 1978).
[39]M. Torfeh and H. Le Gall, Phys. Status Solidi A **63**, 247–258 (1981).